Effective elastic properties of a weakly nonlinear particulate composite

James Vidler[a], Andrei Kotousov[a,*], Ching-Tai Ng[b]

[a] *The University of Adelaide, School of Mechanical Engineering, Adelaide, Australia*
[b] *The University of Adelaide, School of Civil, Environmental & Mining Engineering, Adelaide, Australia*

Abstract

The fundamental problem of finding the effective linear and nonlinear elastic properties of a particulate composite subjected to finite elastic deformations is solved when the matrix and particulate phases are assumed to be weakly nonlinear. Weak nonlinearity is adequate to describe common engineering materials and composites loaded in the elastic regime. A nonlinear analogue of the Eshelby solution for the axisymmetric deformation of spherical particles is derived. Based on this solution, explicit asymptotic expressions for the effective linear and third-order (nonlinear) elastic moduli are derived in the case of a dilute distribution of spherical particles based on a general homogenisation methodology proposed by Hill. It is demonstrated that the current solutions correctly recover well-known relationships for the linear material properties of particulate composites as well as previously derived expressions for the effective nonlinear properties for certain special cases considered previously (e.g. hydrostatic loading, and a neo-Hookean matrix

*Corresponding author.
Email address: andrei.kotousov@adelaide.edu.au (Andrei Kotousov)

containing voids). The obtained theoretical results also agree with limited experimental data available in the literature.
Keywords: finite deformation theory, nonlinear elasticity, particulate composite, spherical particles, effective properties

1. Introduction

In multiphase composites, the presence of secondary phases may influence the mechanical behaviour of the material on the structural scale; therefore, the development of simple and accurate estimates of the effective material properties has been of enduring interest for many decades or even centuries. Beginning with the pioneering studies of Voigt and Reuss [1, 2] on polycrystalline aggregates, many estimates have been proposed for the effective behaviour of multiphase composites. Variational principles have been widely applied to develop strict bounds for linear elasticity, (e.g. the well-known Hashin-Shtrikman [3] bounds); and, in the spirit of the Eshelby solution [4, 5], many averaging methodologies have been developed (e.g. the Mori-Tanaka method [6], the self-consistent [7] and the generalised self-consistent schemes [8] to name a few). However, corresponding results for nonlinear materials subjected to finite deformations are sparse, which is attributable to the inherent mathematical difficulties associated with solving nonlinear problems [9]. When attempting to derive upper and lower bounds, a critical impediment is that the theory of finite deformations features stationary principles, rather than the strict extremum principles of linear elasticity [10]. Meanwhile, for convex and polyconvex incompressible materials, strict bounds have been obtained [11], though these bounds are still not available for compressible

materials. For common structural materials, which are typically modelled as weakly nonlinear, there are as yet no available bounds on the effective material properties.

One approach which has been used to estimate the effective properties of nonlinear composites is based on the concept of the Representative Volume Element (RVE). Subject to an appropriate set of boundary conditions, the effective properties may be derived based on certain averaged properties of the deformation and stress fields in the RVE. As discussed by [12, 13], a widely applied criterion for selecting appropriate boundary conditions is the Hill-Mandel condition, which establishes incremental energy equivalence between the structural scale and the microscopic scale (or the scale of the inhomogeneity) [14]. This approach is suitable for composites with distinct microstructural length scales, and is also well-suited to numerical evaluations of effective material properties using computational procedures and methods e.g. the Finite Element (FE) method. These procedures and methods allow the analysis of complex phase geometries subjected to finite deformations as well as modelling of the interaction between constituents, e.g. the effect of the arrangement, debonding along interfaces, damage caused by fracture of the constituent phases, or cavitation [15]. A number of recent studies have modelled inhomogeneous nonlinear materials using the multi-level FE method [16], the FE method based on asymptotic homogenisation [17], and the weighted essentially non-oscillatory finite difference method [18]. It must be noted that the computational studies cited above did not consider weakly nonlinear materials, which, as mentioned above, best describe the mechanical behaviour of common engineering materials (e.g. metals and alloys) and

composite constituencies subjected to elastic deformation.

Though no systematic studies have been published, it appears that the numerical homogenisation of weakly nonlinear composites presents a significant challenge for current computational procedures and methods, as the nonlinear response in such materials is expected to be several orders of magnitude smaller than the dominant linear response, and may be indistinguishable from errors associated with the selection of the RVE, and its morphology; as well as errors arising from discretisation and numerical precision. As an example, the maximum strain which can be tolerated by common materials without yielding (e.g. steel and aluminium alloys in the elastic regime) is typically 10^{-3}, for which the magnitude of the nonlinear effects would be expected to be of the order 10^{-6}. Therefore, numerical simulations require extensive convergence and mesh sensitivity studies, which can only indirectly indicate the quality and accuracy of the numerical results. In addition, direct numerical simulations often apply periodic boundary conditions [19, 20] implicitly introducing material anisotropy, which requires special treatment or some sort of compensation, which again can be comparable with the effects associated with material nonlinearities. Compliance with all these requirements might be unfeasible, specifically in the case of parametric studies. Overall, it appears that the problem under consideration is more amenable to an analytical rather than numerical treatment.

Several previous studies have investigated nonlinear properties of composite materials using simple constitutive models for incompressible isotropic materials [21]. The number of material constants and, therefore, the complexity of the analysis is greatly reduced in these cases, allowing for closed-

form analytical solutions [22]. For example, Hashin [23] investigated radially symmetric motions of incompressible media containing voids, with particular focus on cavitation and other instabilities. An exact solution for two-dimensional neo-Hookean solids featuring a random microstructure has also been developed [24]. However, as mentioned above, the limited number of exact solutions which are known for physically reasonable constitutive models, and the inherent mathematical difficulties involved in deriving them, represent substantial impediments for analytical treatments. More recently, an effective strain energy function for neo-Hookean and non-Gaussian elastomers weakened by a distribution of spherical voids [20] was derived based on an approximate analytical solution, which was shown to agree well with FE simulations. Based on this study, it was also concluded that the effective properties were relatively insensitive to the distribution and arrangement of voids in the composite material. Subsequent research has revealed that syntactic foams [25], nonlinear viscoelastic materials [26, 27] and thin, perforated plates [28] display a similar property, and provided experimental verification of this phenomenon. However, there is no general theory which would help to identify the situations where the arrangement and distribution of composite constituencies have a small influence on the overall behaviour of the composite.

Most authors have turned to approximate solutions or perturbation methods in order to estimate the effective nonlinear properties. Ogden [9] derived the effective nonlinear compressive modulus for a particulate composite featuring a dilute distribution of spherical particles using volume averaging in combination with a perturbation expansion; the analytical manipulations in

this case are reduced, as the problem is one dimensional. For particulate composites in which the matrix phase may be approximated by a linear material, the Eshelby solution has been generalised to encompass a nonlinear inclusion [29]. Using this approximation, it was possible to present closed-form expressions for the effective nonlinear elastic constants, though the results can only be expected to be valid when the degree of nonlinearity of the matrix is negligible compared to that of the particulate phase. Another interesting method based on a perturbation of the elastic energy density function and Eshelby's solution has recently been presented by Semenov and Beltukov [19] to evaluate the effective nonlinear elastic properties i.e. the third-order elastic constants (TOECs) of a weakly nonlinear particulate composite. These authors derived explicit expressions for the effective properties of particulate composites using the Eshelby equivalence principle [4, 5]. The analytical computations were reduced in this case, as the referential volume average of the elastic strain energy was used in the homogenisation scheme, and the authors were able to use integral transformations to derive effective properties which only depend on the linear elastic solution. The method substantially reduces the complexity of the analytical computations, and the derived effective elastic constants were compared against their own FE simulations demonstrating a very good agreement for dilute distributions of particles, across a wide range of material properties of composite constituencies. However, the obtained analytical expressions do not recover classical results, e.g. the nonlinear compressive effective modulus of neo-Hookean composites containing voids, which had previously been obtained by Hashin [23, 20]; this discrepancy warrants further study.

This paper begins with a brief background on the relevant equations in the finite deformation theory of elasticity. In Section 3 a second-order solution for a RVE of a weakly nonlinear particulate composite is presented and validated by comparison with previous studies. In conjunction with the averaging methodology proposed by Hill, the perturbation solution is used in Section 4 to derive closed-form expressions of the linear and nonlinear elastic properties of particulate composites with random microstructure. It is demonstrated that the present solution recovers previously published results, including the special case of a material containing cavities in Section 5 and the classical result for a neo-Hookean matrix due to Hashin [23]. Additionally, numerical results for composites with properties which have been reported in the literature are presented to reveal characteristic features of the variation of the nonlinear elastic properties with volume fraction of particles. The present theoretical results are also compared with the experimental data found in the literature demonstrating a good agreement. Some implications and possible applications of the derived expressions are presented in Section 6, including the potential to accurately evaluate the concentration of impurities in a material, as well as the amplification or suppression of nonlinear wave phenomena in composite materials.

2. Governing equations

The governing equations of nonlinear elasticity relevant to the problem under consideration are briefly reviewed; a detailed development of the theory may be found in [22, 30]. Consider a body occupying a fixed reference configuration B_r which experiences a deformation given by the mapping $\varphi : B_r \to B$,

where B is the final configuration. Let the reference and final points of a body be given by X and x, respectively. The local properties of the deformation are described by the deformation gradient $\mathbf{F}$, with the component representation

$$F^a_{\ A} = \frac{\partial \varphi^a}{\partial X^A},$$

and the right Cauchy-Green deformation tensor is defined $\mathbf{C} = \mathbf{F}^{\mathrm{T}}\mathbf{F}$. If the body is isotropic and hyperelastic, a strain energy density function W exists, and the second Piola-Kirchhoff stress tensor $\mathbf{S}$ may be expressed in terms of $\mathbf{C}$, its principal invariants I_1, I_2, I_3, and the metric tensor of the reference coordinate system $\mathbf{G}$,

$$\mathbf{S} = 2\left(\frac{\partial W}{\partial I_1} + I_1\frac{\partial W}{\partial I_2}\right)\mathbf{G} - 2\frac{\partial W}{\partial I_2}\mathbf{C} + 2I_3\frac{\partial W}{\partial I_3}\mathbf{C}^{-1} \tag{1}$$

where the invariants are

$$I_1 = \mathrm{tr}(\mathbf{C})\,, \quad I_2 = \det\mathbf{C}\,\mathrm{tr}(\mathbf{C}^{-1})\,, \quad I_3 = \det\mathbf{C}.$$

The first Piola-Kirchhoff stress tensor $\mathbf{P}$ is related to $\mathbf{S}$ via $\mathbf{P} = \mathbf{F}\mathbf{S}$. In the absence of body forces, the equations of equilibrium in terms of the first Piola-Kirchhoff stress tensor are

$$\mathrm{Div}\,\mathbf{P} = \mathbf{0} \tag{2}$$

where the divergence is taken with respect to the coordinate system of the material points. The third-order expansion of the strain energy density function [31] for a compressible, isotropic material is

$$\begin{aligned} W(I_1, I_2, I_3) = {} & \tfrac{1}{8}(\lambda + 2\mu)(I_1 - 3)^2 - \tfrac{1}{2}\mu(I_2 - 2I_1 + 3) + \tfrac{1}{24}(l + 2m)(I_1 - 3)^3 \\ & - \tfrac{1}{4}m(I_1 - 3)(I_2 - 2I_1 + 3) + \tfrac{1}{8}n(I_1 - I_2 + I_3 - 1) \end{aligned} \tag{3}$$

where the linear elastic constants are the Lamé parameters λ and μ, and the TOECs are l, m and n, expressed in Murnaghan's form. It is also common to express the TOECs using the equivalent Landau-Lifshitz constants A, B, C, where

$$A = n\,, \quad B = m - \tfrac{1}{2}n\,, \quad C = l - m + \tfrac{1}{2}n. \tag{4}$$

2.1. Problem statement

In the particulate composite medium under consideration, the radii of the embedded particles are assumed to be much smaller than the macroscopic dimensions of the composite medium, and dilutely distributed; this condition establishes a strict separation of length scales, and therefore analysis of the macroscopic material may be achieved using a RVE. For a dilute particulate composite medium, under the assumption of a strict separation of length scales, the interaction between particles may be ignored, and the RVE has the form of a spherical shell [32, 13].

In accordance with the Hill-Mandel condition, if the external boundary of the macroscopic medium is subjected to linear displacement conditions, then identical conditions must be applied to the external boundary of the RVE to establish incremental energy equivalence [14]. The averaging scheme proposed by Hill [12, 13] asserts that the referential volume average of both the deformation gradient $\mathbf{F}$ and the first Piola-Kirchhoff stress $\mathbf{P}$ are consistent between the macroscopic material and the RVE. A detailed explanation of the methodology was given by Ogden [9].

Therefore, the effective elastic properties of the composite medium under consideration may be estimated based on the solution to the following problem: given the composite sphere shown in Fig. 1 with initial particle

volume fraction $f_0 = R_i^3/R_e^3$ subjected to a given surface deformation, determine the accompanying displacement and stress distributions within the volume. Each constituent phase is described by the Murnaghan strain energy function (3). The elastic constants of the inhomogeneity are denoted λ_p, μ_p, l_p, m_p, n_p; the elastic constants of the matrix are denoted λ_m, μ_m, l_m, m_m, n_m. The derived distributions may be used in conjunction with a homogenisation methodology to estimate the effective third-order elastic constants of a weakly nonlinear particulate composite. The magnitude of the deformations applied to the composite are assumed to be limited such that each constituent may be modelled as a weakly nonlinear elastic material, with strain energy density functions of the form (3).

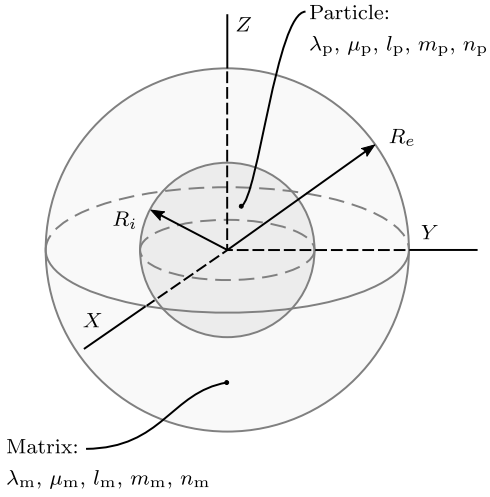

Figure 1: Representative volume element for the composite medium. The external boundary $R = R_e$ is subjected to linear displacement conditions which are axisymmetric with respect to the Z axis.

Due to the isotropic properties of both phases, and the random distribution of the inhomogeneities, the macroscopic material may be assumed to be

isotropic. Hence the strain energy function of the composite medium may be taken in the form (3) with the effective elastic constants of the composite medium as λ_{eff}, μ_{eff}, l_{eff}, m_{eff} and n_{eff}, and the comparison material takes the form shown in Fig. 2.

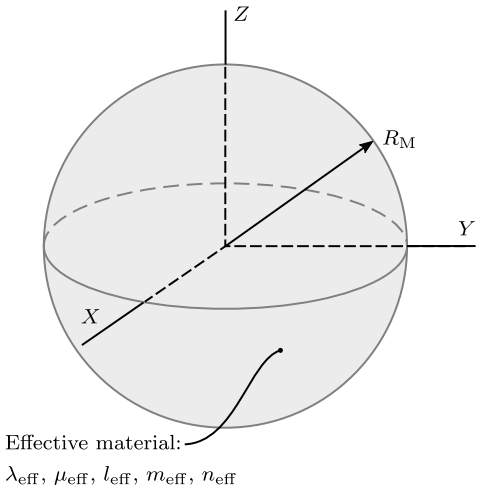

Figure 2: Effective macroscopic body, subjected to linear displacement boundary conditions which are equivalent to the RVE boundary conditions.

In the macroscopic material, the referential volume averages of the deformation gradient, $\overline{\mathbf{F}}$, and the first Piola-Kirchhoff stress, $\overline{\mathbf{P}}$, may be calculated using volume integrals, and the methodology states that

$$\frac{1}{V}\int_V \mathbf{F}\, dV = \overline{\mathbf{F}} \tag{5a}$$

$$\frac{1}{V}\int_V \mathbf{P}\, dV = \overline{\mathbf{P}}. \tag{5b}$$

where the volume integrals on the left side of the above equations are the referential volume averages, expressed in a Cartesian basis, of the deformation gradient and the first Piola-Kirchhoff stress in the RVE. Finally, the effective elastic constants are determined by solving eqs. (5a) and (5b).

2.2. Problem formulation

For general anisotropic materials, the nature of the boundary deformation necessary to extract all the independent effective elastic constants must be highly general; however, due to the macroscopic isotropy of the particulate composite medium under consideration in this study, it suffices to consider displacement conditions on the external boundary $R = R_e$ which are axisymmetric with respect to the polar axis Z. This assumption also substantially simplifies the analysis. The appropriate axisymmetric boundary condition is

$$\mathbf{z}(R_e) - \mathbf{Z}(R_e) = U(\alpha X \mathbf{d}_X + \alpha Y \mathbf{d}_Y + Z \mathbf{d}_Z) \tag{6}$$

where $\mathbf{z}$ and $\mathbf{Z}$ denote the position vectors of referential and spatial points, respectively; U and α are parameters characterising the deformation; and $\mathbf{d}_X$, $\mathbf{d}_Y$, $\mathbf{d}_Z$ form an orthonormal Cartesian basis, with the Z coordinate aligned with the axis of symmetry. The parameter α controls the degree of lateral contraction, varying between a radially symmetric motion when $\alpha = 1$, a simple extension without lateral contraction when $\alpha = 0$. It is also necessary to impose continuity conditions on the displacement and first Piola-Kirchhoff traction across phase interfaces,

$$\mathbf{z}^{(m)}(R_i) - \mathbf{z}^{(p)}(R_i) = \mathbf{0} \tag{7a}$$

$$(\mathbf{P}^{(m)} - \mathbf{P}^{(p)})\mathbf{d}_R = \mathbf{0}\,, \quad R = R_i \tag{7b}$$

where $\mathbf{d}_R$ is the radial basis vector in the material configuration.

To identify the effective elastic constants of the composite medium using eqs. (5a) and (5b) it is necessary to identify the volume average over the referential body of both the deformation gradient and the first Piola-Kirchhoff

stress. The Stokes theorem may be used in conjunction with eq. (6) to show that, irrespective of the details of the internal stress and strain fields,

$$\frac{1}{V}\int_V \mathbf{F}\,dV = \frac{1}{V}\oint_{\partial V} \mathbf{z}\otimes\mathbf{n}\,dS \tag{8}$$

providing $\overline{\mathbf{F}} = \mathrm{diag}(1+U\alpha, 1+U\alpha, 1+U)$ with respect to a Cartesian basis. The calculation of the referential volume average of the first Piola-Kirchhoff stress however, requires the solution of the elasticity problem, which is discussed in the following Section.

3. Axisymmetric solution for single inclusion

As discussed in Section 1, an analysis of the macroscopic behaviour of the particulate composite material may be undertaken based on a RVE, for which the geometry and formulation of the elasticity problem has been described in Sections 2.1 and 2.2. The present state of knowledge in nonlinear elasticity does not permit an exact analytical solution for the problem as formulated. However, approximate solutions may be derived using perturbation methods. Applied to the present nonlinear elasticity problem, the perturbation method assumes that the magnitude of the displacements are sufficiently small that the governing equations may be expanded as series; the resulting equations provide a hierarchy of linear elasticity problems which may be solved sequentially (for examples, see [30, 33]). It is important to note that while the assumptions involved in the perturbation solution imply that the results will be less accurate for large deformations, the results should be sufficient to represent the response of common engineering materials loaded in the elastic regime.

3.1. Perturbation solution

Applying the perturbation method to the axisymmetric problem described in Section 2.1, the deformation φ may be represented using the spherical coordinates (R, Θ, Φ) and (r, θ, ϕ) for the material and spatial frames respectively. The boundary condition (6) may be expanded as a power series with respect to the magnitude of the displacement U in the boundary condition (6), providing

$$\mathbf{z} - \mathbf{Z} = U\mathbf{u}_1 + U^2\mathbf{u}_2. \tag{9}$$

The condition $U \ll 1$ is assumed to ensure the validity of the perturbation expansion, and the vectors $\mathbf{u}_1$ and $\mathbf{u}_2$ represent the first-order and second-order displacement vectors, respectively. For axisymmetric deformations, $r = r(R, \Theta)$, $\theta = \theta(R, \Theta)$, $\phi = \Phi$ and the displacement vectors are

$$\mathbf{u}_1 = u_R^{(1)}(R, \Theta)\mathbf{d}_R + u_\Theta^{(1)}(R, \Theta)\mathbf{d}_\Theta \tag{10a}$$

$$\mathbf{u}_2 = u_R^{(2)}(R, \Theta)\mathbf{d}_R + u_\Theta^{(2)}(R, \Theta)\mathbf{d}_\Theta \tag{10b}$$

where the basis vectors $\mathbf{d}_R$ and $\mathbf{d}_\Theta$ are given in Appendix A. Using equations (9) and (10), the expansions for the functions $r(R, \Theta)$ and $\theta(R, \Theta)$ in terms of the displacement components are

$$r(R, \Theta) = R + Uu_R^{(1)}(R, \Theta) + U^2\left(u_R^{(2)}(R, \Theta) + \frac{[u_\Theta^{(1)}(R, \Theta)]^2}{2R}\right)$$

$$\theta(R, \Theta) = \Theta + U\frac{u_\Theta^{(1)}(R, \Theta)}{R} + U^2\left(\frac{u_\Theta^{(2)}(R, \Theta)}{R} - \frac{u_R^{(1)}(R, \Theta)u_\Theta^{(1)}(R, \Theta)}{R^2}\right).$$

The first Piola-Kirchhoff stress tensor may be derived from eq. (3) in terms of the Lagrangian strain tensor $\mathbf{E} = \frac{1}{2}(\mathbf{C} - \mathbf{G})$ and its principal invariants $I_1(\mathbf{E})$, $I_2(\mathbf{E})$, $I_3(\mathbf{E})$. Up to second order in the displacement gradient,

$$\mathbf{P} = \lambda I_1(\mathbf{E})\mathbf{F} + 2\mu\mathbf{F}\mathbf{E} + lI_1(\mathbf{E})^2\mathbf{G} + (n-2m)(I_2(\mathbf{E})\mathbf{G} - I_1(\mathbf{E})\mathbf{E}) + n\mathbf{E}^2 + \dots \tag{11}$$

where $\mathbf{G}$ is the metric tensor of the material coordinate system [30]. To facilitate the use of a perturbation scheme, the first Piola-Kirchhoff stress may be rewritten in the form

$$\mathbf{P} = U\boldsymbol{\sigma}(\mathbf{u}_1) + U^2[\boldsymbol{\sigma}(\mathbf{u}_2) + \mathbf{T}'(\mathbf{u}_1)] + \dots \tag{12}$$

where $\boldsymbol{\sigma}(\mathbf{u})$ is the stress tensor of isotropic linear elasticity,

$$\boldsymbol{\sigma}(\mathbf{u}) = \lambda(\operatorname{Div}\mathbf{u})\mathbf{G} + \mu\left(\nabla\mathbf{u} + (\nabla\mathbf{u})^T\right)$$

and $\mathbf{T}'(\mathbf{u}_1)$ represents the second-order correction to the linear stress tensor [34], and is provided in full in Appendix B.

Using these relations, the equilibrium condition (2) may be expanded to provide the familiar equilibrium equations of isotropic linear elasticity, as well as a second-order condition,

$$\operatorname{Div}\boldsymbol{\sigma}(\mathbf{u}_1) = \mathbf{0} \tag{13a}$$

$$\operatorname{Div}\left[\boldsymbol{\sigma}(\mathbf{u}_2) + \mathbf{T}'(\mathbf{u}_1)\right] = \mathbf{0}. \tag{13b}$$

Note that eq. (13b) is identical in form to eq. (13a), apart from the addition of inhomogeneous terms which depend upon $\mathbf{u}_1$. Therefore, the second-order displacement $\mathbf{u}_2$ has the form $\mathbf{u}_2 = \mathbf{u}_2^{(h)} + \mathbf{u}_2'$ where $\mathbf{u}_2^{(h)}$ is a homogeneous solution to eq. (13b), and $\mathbf{u}_2'$ is a particular solution constructed to satisfy

$$\operatorname{Div}\boldsymbol{\sigma}(\mathbf{u}_2') = -\operatorname{Div}\mathbf{T}'(\mathbf{u}_1). \tag{14}$$

Using the strain energy function (3), eq. (13) may be expressed in the form

$$\mu\nabla^2\mathbf{u}_1 + (\lambda+\mu)\nabla\mathrm{Div}\,\mathbf{u}_1 = \mathbf{0} \tag{15a}$$

$$\mu\nabla^2\mathbf{u}_2^{(h)} + (\lambda+\mu)\nabla\mathrm{Div}\,\mathbf{u}_2^{(h)} = \mathbf{0}. \tag{15b}$$

Note that eqs. (15) apply to both the matrix and the particulate phases. The equations in the perturbation expansion of the continuity condition (7a) are

$$\mathbf{u}_1^{(m)}(R_i) - \mathbf{u}_1^{(p)}(R_i) = \mathbf{0} \tag{16a}$$

$$\mathbf{u}_2^{(m)}(R_i) - \mathbf{u}_2^{(p)}(R_i) = \mathbf{0} \tag{16b}$$

where a superposed m is used to indicate a field associated with the matrix phase, while a superposed p indicate the particulate phase. For eq. (7b),

$$[\boldsymbol{\sigma}^{(m)}(\mathbf{u}_1^{(m)}) - \boldsymbol{\sigma}^{(p)}(\mathbf{u}_1^{(p)})]\mathbf{d}_R = \mathbf{0} \tag{17a}$$

$$[\boldsymbol{\sigma}^{(m)}(\mathbf{u}_2^{(m)}) - \boldsymbol{\sigma}^{(p)}(\mathbf{u}_2^{(p)})]\mathbf{d}_R = -\left[\mathbf{T}'^{(m)}(\mathbf{u}_1^{(m)}) - \mathbf{T}'^{(p)}(\mathbf{u}_1^{(p)})\right]\mathbf{d}_R \tag{17b}$$

where $\boldsymbol{\sigma}^{(m)}$ and $\boldsymbol{\sigma}^{(p)}$ denote the stress tensors of isotropic linear elasticity for the matrix and particulate phase, respectively. Finally, the boundary condition (6) leads to the following boundary conditions for the linear and second-order problems:

$$\mathbf{u}_1^{(m)}(R_e) = \tfrac{1}{2}R_e[1+\alpha+(1-\alpha)\cos 2\Theta]\mathbf{d}_R - \tfrac{1}{2}R_e(1-\alpha)\sin 2\Theta\mathbf{d}_\Theta \tag{18a}$$

$$\mathbf{u}_2^{(m)}(R_e) = \mathbf{0}. \tag{18b}$$

Using the perturbation expansion, the nonlinear elastic problem has been reduced to two sequential linear elasticity problems, presented in eqs. (15-18), which may be solved using standard techniques.

3.2. Linear solution

The linear solution to the axisymmetric deformation of a spherical shell containing an isolated spherical inhomogeneity is a standard problem in elasticity, which may be solved using potential functions [35]. The displacement solution is constructed using axisymmetric potential functions for isotropic materials,

$$\mathbf{u}_1^{(m)} = \frac{1}{2\mu_m}\nabla(\chi^{(m)} + Z\eta^{(m)}) - \frac{2(1-\nu_m)}{\mu_m}\eta^{(m)}\mathbf{d}_Z \tag{19}$$

where $\chi^{(m)}$ and $\eta^{(m)}$ are potential functions which can be represented in terms of the axisymmetric spherical harmonic functions. The potentials $\chi^{(m)}$ and $\eta^{(m)}$ which are consistent with the continuity conditions (16a) and (17a), and the boundary condition (18a) are

$$\chi^{(m)} = F_0^{(m)}R_i^3R^{-1} + (A_2^{(m)}R^2 + F_2^{(m)}R_i^5R^{-3})P_2(\cos\Theta) + A_4^{(m)}R_i^{-2}R^4P_4(\cos\Theta) \tag{20a}$$

$$\eta^{(m)} = (B_1^{(m)}R + G_1^{(m)}R_i^3R^{-2})P_1(\cos\Theta) + B_3^{(m)}R_i^{-2}R^3P_3(\cos\Theta) \tag{20b}$$

where $P_n(\cos\Theta)$ is the zonal spherical harmonic of degree n and $F_0^{(m)}, A_2^{(m)}$ etc. are coefficients to be determined. The linear solution for the inhomogeneity phase may be found similarly, though the requirement that the displacement vanishes at the centre of the inhomogeneity imposes a further condition on the solution, and removes terms which are singular at $R = 0$ from the stress and the displacement. Therefore, the linear solution for the displacement in the particulate phase is

$$\mathbf{u}_1^{(p)} = \frac{1}{2\mu_p}\nabla(\chi^{(p)} + Z\eta^{(p)}) - \frac{2(1-\nu_p)}{\mu_p}\eta^{(p)}\mathbf{d}_Z \tag{21}$$

where the potentials are

$$\chi^{(p)} = A_2^{(p)} R^2 P_2(\cos\Theta) + A_4^{(p)} R_i^{-2} R^4 P_4(\cos\Theta) \tag{22a}$$

$$\eta^{(p)} = B_1^{(p)} R P_1(\cos\Theta) + B_3^{(p)} R_i^{-2} R^3 P_3(\cos\Theta). \tag{22b}$$

The coefficients in eqs. (20) and (22) which satisfy the boundary conditions (16a), (17a) and (18a) are provided in Appendix C.

3.3. Second-order solution

The second-order component of the solution consists of a linear elasticity problem for $\mathbf{u}_2$ featuring a body force distribution and surface traction dependent on the linear solution $\mathbf{u}_1$. As discussed in Section 3.1, the second-order displacement in the matrix phase may be represented as $\mathbf{u}_2^{(m)} = \mathbf{u}_2^{(m,h)} + \mathbf{u}_2^{\prime(m)}$. The homogeneous solution has the form

$$\mathbf{u}_2^{(m,h)} = \frac{1}{2\mu_m} \nabla(\chi_2^{(m)} + Z\eta_2^{(m)}) - \frac{2(1-\nu_m)}{\mu_m} \eta_2^{(m)} \mathbf{d}_Z \tag{23}$$

where, as with the linear solution, the potentials $\chi_2^{(m)}$ and $\eta_2^{(m)}$ are constructed using axisymmetric spherical harmonic functions

$$\begin{aligned}\chi_2^{(m)} = {} & F_1^{(m)} R_i^3 R^{-1} + (A_3^{(m)} R^2 + F_3^{(m)} R_i^5 R^{-3}) P_2(\cos\Theta) \\ & + (A_5^{(m)} R_i^{-2} R^4 + F_5^{(m)} R_i^7 R^{-5}) P_4(\cos\Theta) + A_7^{(m)} R_i^{-4} R^6 P_6(\cos\Theta)\end{aligned} \tag{24a}$$

$$\begin{aligned}\eta_2^{(m)} = {} & (B_2^{(m)} R + G_2^{(m)} R_i^3 R^{-2}) P_1(\cos\Theta) + (B_4^{(m)} R_i^{-2} R^3 + G_4^{(m)} R_i^5 R^{-4}) P_3(\cos\Theta) \\ & + B_6^{(m)} R_i^{-4} R^5 P_5(\cos\Theta).\end{aligned} \tag{24b}$$

The particular solution may be constructed using a scalar function ζ and a vector function $\mathbf{w}$ [36], related to the displacement via

$$\mathbf{u}_2^{\prime(m)} = \frac{1}{2\mu_m} \nabla\zeta^{(m)} - \frac{2(1-\nu_m)}{\mu_m} \nabla^2 \mathbf{w}^{(m)} + \frac{1}{\mu_m} \nabla \mathrm{Div}\, \mathbf{w}^{(m)}. \tag{25}$$

The forms of $\zeta^{(m)}$ and $\mathbf{w}^{(m)}$ depend on the linear elasticity solution $\mathbf{u}_1^{(m)}$, and may be derived using eq. (14). Full expressions are provided in Appendix D.1.

Similarly, the second-order solution for the particulate phase is $\mathbf{u}_2^{(p)} = \mathbf{u}_2^{(p,h)} + \mathbf{u}_2^{\prime(p)}$. The homogeneous solution is

$$\mathbf{u}_2^{(p,h)} = \frac{1}{2\mu_p}\nabla(\chi_2^{(p)} + Z\eta_2^{(p)}) - \frac{2(1-\nu_p)}{\mu_p}\eta_2^{(p)}\mathbf{d}_Z \tag{26}$$

where the second-order potentials are

$$\chi_2^{(p)} = A_3^{(p)}R^2P_2(\cos\Theta) + A_5^{(p)}R_i^{-2}R^4P_4(\cos\Theta) + A_7^{(p)}R_i^{-4}R^6P_6(\cos\Theta) \tag{27a}$$

$$\eta_2^{(p)} = B_2^{(p)}RP_1(\cos\Theta) + B_4^{(p)}R_i^{-2}R^3P_3(\cos\Theta) + B_6^{(p)}R_i^{-4}R^5P_5(\cos\Theta) \tag{27b}$$

and the particular solution is

$$\mathbf{u}_2^{\prime(p)} = \frac{1}{2\mu_p}\nabla\zeta^{(p)} - \frac{2(1-\nu_p)}{\mu_p}\nabla^2\mathbf{w}^{(p)} + \frac{1}{\mu_p}\nabla\mathrm{Div}\,\mathbf{w}^{(p)} \tag{28}$$

where the scalar function $\zeta^{(p)}$ and the vector $\mathbf{w}^{(p)}$ associated with the second-order solution are presented in Appendix D.2.

3.4. Summary of perturbation solution

The linear elasticity problem given by eqs. (15a), (16a), and (17a) leads to a system of linear algebraic equations for the coefficients in eqs. (20) and (22), provided in Appendix C.

For the second-order solution, the potentials $\zeta^{(m)}$, $\zeta^{(p)}$ and the vectors $\mathbf{w}^{(m)}$, $\mathbf{w}^{(p)}$ are presented in Appendix D. Finally, eqs. (16b), (17b) and (18b) may be used to calculate the coefficients in eqs. (24) and (27). Though the resulting expressions are extremely lengthy, the calculation is routine in

linear elasticity: for this reason, expressions for each coefficient in the second-order solution are provided in the form of a Python code as supplementary data. Example values of each coefficient are provided in Appendix E.

The analytic second-order solution derived above may be compared to other solutions in the literature. The second-order solution for spherically-symmetric motions of a composite sphere presented by Ogden [9] may be recovered by applying the condition $\alpha = 1$. Similarly, the second-order solution for an infinite medium containing an isolated spherical cavity presented in [37] may be recovered using the limiting conditions $R_e \to \infty$ and setting the elastic constants of the inhomogeneity to zero.

4. Effective elastic properties of composites

The second-order elasticity problem formulated in Section 2 and solved in Section 3 may be used to estimate the effective elastic constants of a composite consisting of a distribution of spherical particles embedded in a matrix. In this work, a methodology proposed by Hill [12], based on equating the field quantities averaged over a representative volume, is used.

For a two-phase composite, eqs. (5a) and (5b) have the form

$$\frac{1}{V}\int_V \mathbf{F}\, dV = \frac{1}{V}\int_{V_m} \mathbf{F}^{(m)}\, dV + \frac{1}{V}\int_{V_p} \mathbf{F}^{(p)}\, dV \tag{29a}$$

$$\frac{1}{V}\int_V \mathbf{P}\, dV = \frac{1}{V}\int_{V_m} \mathbf{P}^{(m)}\, dV + \frac{1}{V}\int_{V_p} \mathbf{P}^{(p)}\, dV. \tag{29b}$$

where V_m is the spherical shell $R_i < R < R_e$, and V_p is the sphere $R < R_i$. Applied to the results obtained in Sections 3.2 and 3.3, the above equations may be used to estimate the effective linear elastic constants and the TOECs of a composite material containing spherical inhomogeneities.

4.1. Macroscopic material

The macroscopic body is a sphere of outer radius R_{M} (see Fig. 2), described by the strain energy function (3), with uniform material properties λ_{eff}, μ_{eff}, l_{eff}, m_{eff}, n_{eff}. The macroscopic body is subjected to the linear displacement boundary condition (6).

As the macroscopic body is an isotropic body of uniform material properties subjected to a homogeneous strain, an analytical solution is possible [30]. Applying uniform, axisymmetric stretches $\lambda_1 = \lambda_2$, λ_3 such that $\overline{\mathbf{F}} = \mathrm{diag}(\lambda_1, \lambda_1, \lambda_3)$, the first Piola-Kirchhoff stress tensor is calculated using eq. (1),

$$\begin{aligned}
\overline{\mathbf{P}} &= \mathrm{diag}(\overline{P}_{11}, \overline{P}_{11}, \overline{P}_{33}) \\
\overline{P}_{11} &= \lambda_1 \left[\tfrac{1}{2}\lambda_{\mathrm{eff}}(2\lambda_1^2 + \lambda_3^2 - 3) + \mu_{\mathrm{eff}}(\lambda_1^2 - 1) + \tfrac{1}{4}l_{\mathrm{eff}}(2\lambda_1^2 + \lambda_3^2 - 3)^2 \right. \\
&\qquad \left. -\tfrac{1}{2}m_{\mathrm{eff}}(\lambda_3^2 - \lambda_1^2)(\lambda_1^2 - 1) + \tfrac{1}{4}n_{\mathrm{eff}}(\lambda_1^2 - 1)(\lambda_3^2 - 1)\right] \\
\overline{P}_{33} &= \lambda_3 \left[\tfrac{1}{2}\lambda_{\mathrm{eff}}(2\lambda_1^2 + \lambda_3^2 - 3) + \mu_{\mathrm{eff}}(\lambda_3^2 - 1) + \tfrac{1}{4}l_{\mathrm{eff}}(2\lambda_1^2 + \lambda_3^2 - 3)^2 \right. \\
&\qquad \left. +\tfrac{1}{2}m_{\mathrm{eff}}(\lambda_3^2 - \lambda_1^2)(\lambda_1^2 + \lambda_3^2 - 2) + \tfrac{1}{4}n_{\mathrm{eff}}(\lambda_1^2 - 1)\right].
\end{aligned}$$

Rewriting the stretches in terms of the linear displacement boundary condition 6, $\lambda_1 = \lambda_2 = 1 + U\alpha$, $\lambda_3 = 1 + U$, the components of the macroscopic first Piola Kirchhoff stress tensor, expanded as series in U, are

$$\begin{aligned}
\overline{P}_{11} &= U[(1+2\alpha)\lambda_{\mathrm{eff}} + 2\alpha\mu_{\mathrm{eff}}] \\
&\quad + U^2\left[(\tfrac{1}{2} + \alpha + 3\alpha^2)\lambda_{\mathrm{eff}} + 3\alpha^2\mu_{\mathrm{eff}} + (1+2\alpha)^2 l_{\mathrm{eff}} + 2\alpha(\alpha-1)m_{\mathrm{eff}} + \alpha n_{\mathrm{eff}}\right] + \ldots
\end{aligned} \tag{30a}$$

$$\begin{aligned}
\overline{P}_{33} &= U[(1+2\alpha)\lambda_{\mathrm{eff}} + 2\mu_{\mathrm{eff}}] \\
&\quad + U^2\left[(\tfrac{3}{2} + 2\alpha + \alpha^2)\lambda_{\mathrm{eff}} + 3\mu_{\mathrm{eff}} + (1+2\alpha)^2 l_{\mathrm{eff}} + 2(1-\alpha^2)m_{\mathrm{eff}} + \alpha^2 n_{\mathrm{eff}}\right] + \ldots
\end{aligned} \tag{30b}$$

with $\overline{P}_{22} = \overline{P}_{33}$.

4.2. Effective elastic constants

Returning to the problem described in Section 3, the referential volume average of the deformation gradient and the first Piola-Kirchhoff stress tensor may now be calculated. As discussed in Section 2.2, the boundary condition (6) and the identity (8) imply that $\overline{\mathbf{F}} = \mathrm{diag}(1 + U\alpha, 1 + U\alpha, 1 + U)$ and eq. (5a) is automatically satisfied.

The perturbation method allows the average first Piola-Kirchhoff stress tensor for the RVE to be expressed as a series:

$$\overline{\mathbf{P}} = U\overline{\mathbf{P}^{(1)}} + U^2\overline{\mathbf{P}^{(2)}} + \dots \tag{31}$$

where $\overline{\mathbf{P}^{(1)}}$ and $\overline{\mathbf{P}^{(2)}}$ are the averaged stress distributions accompanying the linear and second-order elastic solutions, respectively. The components corresponding to the linear elastic solution are

$$\overline{P_{11}^{(1)}} = -A_2^{(m)} - \frac{\lambda_m}{\lambda_m + \mu_m} B_1^{(m)} - \frac{3}{5} f_0^{-2/3} B_3^{(m)} + 2 f_0 F_0^{(m)} + \frac{7\lambda_m + 12\mu_m}{5(\lambda_m + \mu_m)} f_0 G_1^{(m)} \tag{32a}$$

$$\overline{P_{33}^{(1)}} = 2A_2^{(m)} - \frac{\lambda_m + 2\mu_m}{\lambda_m + \mu_m} B_1^{(m)} + \frac{6}{5} f_0^{-2/3} B_3^{(m)} + 2 f_0 F_0^{(m)} + \frac{16\lambda_m + 26\mu_m}{5(\lambda_m + \mu_m)} f_0 G_1^{(m)} \tag{32b}$$

and the averaged second-order components may be derived using the expansion (12) in combination with the expressions for the coefficients of the displacement potentials in the second-order elastic solution (see Appendix E and the supplementary data). Due to the length of the resulting expressions, the full forms are omitted.

Using the linear terms in eqs. (5b), (30) and (32), the effective linear elastic constants are

$$K_{\text{eff}} = \frac{3K_mK_p + 4\mu_m[(1-f_0)K_m + f_0K_p]}{4\mu_m + 3[f_0K_m + (1-f_0)K_p]} \tag{33a}$$

$$\mu_{\text{eff}} = \mu_m \frac{6\mu_p(K_m + 2\mu_m) + (9K_m + 8\mu_m)[(1-f_0)\mu_m + f_0\mu_p]}{\mu_m(9K_m + 8\mu_m) + 6(K_m + 2\mu_m)[f_0\mu_m + (1-f_0)\mu_p]} \tag{33b}$$

in agreement with previous studies conducted within the theory of linear elasticity [38]. To simplify the equations for the TOECs, it is convenient to introduce the notations $q = l + \frac{1}{9}n$ and $s = m - \frac{1}{6}n$. The TOEC q is a second-order analogue of the bulk modulus K, though s and n are not, to the best knowledge of the authors, amenable to such a simple, physical interpretation. The effective second-order bulk modulus $q_{\text{eff}} = l_{\text{eff}} + \frac{1}{9}n_{\text{eff}}$, derived by considering a spherically symmetric motion (i.e. $\alpha = 1$), is

$$\begin{aligned} q_{\text{eff}} = {} & (1-f_0)q_m + f_0q_p + \frac{9(1-f_0)(K_{\text{eff}} - K_m)(q_m - q_p)}{3K_m + 4\mu_m} \\ & + \frac{9(1-f_0)(K_{\text{eff}} - K_m)^2(3K_m + 4s_m + 6[f_0q_m + (1-f_0)q_p])}{2f_0(3K_m + 4\mu_m)^2} \\ & + \frac{3(1-f_0)(K_{\text{eff}} - K_m)^3}{2f_0^2(3K_m + 4\mu_m)^3}\Big[18\mu_m + 2n_m + f_0(27K_{\text{m}} + 18\mu_m + 36s_m + 2n_m) \\ & \qquad + 18f_0^2q_m - 18(1-f_0)^2q_p\Big]. \end{aligned} \tag{34}$$

This result for the effective second-order bulk modulus of a compressible composite medium presented agrees with the first-order expansion in f_0 presented in [9].

For the other TOECs, expressions valid for all values of the volume fraction f_0 are extremely cumbersome, though a detailed analysis of the full expressions reveals that the choice of the TOECs q, s and n provides some

simplification in the resulting expressions. In particular, q_{eff} is independent of s_p and n_p; similarly, s_{eff} is independent of n_p. In spite of the length of the complete expressions, fairly compact series expansions in terms of f_0 may be derived; in terms of q, s and n, the Taylor expansions of the remaining effective TOECs are

$$\begin{aligned} s_{\text{eff}} = s_m + f_0 \Bigg[& \frac{25\mu_m^2(3K_m + 4\mu_m)^3}{h_0 k_0^2} s_p + \frac{120\mu_m^2(\mu_p - \mu_m)^2}{k_0^2} q_m + \frac{2(\mu_p - \mu_m)}{h_0 k_0^2} p_{2,0} \\ & + \frac{(K_p - K_m)(\mu_p - \mu_m)}{2h_0 k_0^2} p_{1,0} n_m + \frac{1}{h_0 k_0^2} p_{3,1} s_m \\ & - \left(\frac{1}{h_0 k_0^2} - \frac{3(K_p - K_m)}{h_0^2 k_0^2} - \frac{12(K_m + 2\mu_m)(\mu_p - \mu_m)}{h_0 k_0^3} \right) p_{3,0} s_m \Bigg] \end{aligned} \tag{35a}$$

$$\begin{aligned} n_{\text{eff}} = n_m + f_0 \Bigg[& \frac{125\mu_m^3(3K_m + 4\mu_m)^3}{k_0^3} n_p + \frac{7200\mu_m^3(\mu_p - \mu_m)^3}{7k_0^3} q_m - \frac{60\mu_m(\mu_p - \mu_m)^2}{7k_0^3} p_{4,0} \\ & + \frac{180\mu_m(\mu_p - \mu_m)^2}{7k_0^3} p_{1,0} s_m + \frac{1}{7k_0^3} p_{5,1} n_m \\ & + \left(\frac{18(K_m + 2\mu_m)(\mu_p - \mu_m)}{7k_0^4} - \frac{1}{7k_0^3} \right) p_{5,0} n_m \Bigg] \end{aligned} \tag{35b}$$

where the constants h_0, k_0, $p_{1,0}$, $p_{2,0}$, $p_{3,0}$, $p_{3,1}$ are presented in Appendix F. As mentioned above, exact expressions for the effective TOECs s_{eff} and n_{eff} are extremely lengthy. Complete expressions suitable for evaluation in Python are provided as supplementary data.

5. Discussion

5.1. Incompressible matrix containing voids

The effective elastic constants of a neo-Hookean incompressible material containing a distribution of spherical voids may be obtained from the present results as a limiting case. First, the particle phase is reduced to a distribution of voids using the following limits

$$\lambda_p \to 0\,, \quad \mu_p \to 0\,, \quad l_p \to 0\,, \quad m_p \to 0\,, \quad n_p \to 0. \tag{36}$$

The compressible matrix may be converted to a third-order incompressible matrix with the strain energy function

$$W_{\mathrm{I},3} = \mu\,\mathrm{tr}\mathbf{E}^2 + \frac{1}{3}A\,\mathrm{tr}\mathbf{E}^3 \tag{37}$$

using the incompressible limits provided by [39],

$$(1-2\nu)B \to -\mu\,, \quad (1-2\nu)^3 C \to 0 \tag{38}$$

where A, B, and C are the Landau-Lifshitz constants, see eq. (4). Finally, the case of a neo-Hookean material is recovered by setting $A = -4\mu$. The corresponding effective linear elastic constants are

$$\mu_{\mathrm{eff}} = \frac{(1-f_0)\mu}{1+\frac{2}{3}f_0} \tag{39a}$$

$$K_{\mathrm{eff}} = \frac{4(1-f_0)\mu}{3f_0} \tag{39b}$$

and the effective second-order bulk modulus is

$$l_{\mathrm{eff}} + \tfrac{1}{9}n_{\mathrm{eff}} = -\frac{(1-f_0)(11+15f_0)}{9f_0^2}\mu_m. \tag{40}$$

The remaining effective TOECs are extremely lengthy, and are provided as supplementary data in the form of a Python code.

For a neo-Hookean incompressible material containing a distribution of spherical voids, there is only one non-zero independent elastic constant for the constituents, namely the shear modulus of the matrix μ_m; but the macroscopic composite features three effective moduli, and exhibits macroscopic compressibility due to the presence of pores as found by [23]. The variations in the effective nonlinear elastic constants for a neo-Hookean material with spherical voids are shown in Fig. 3.

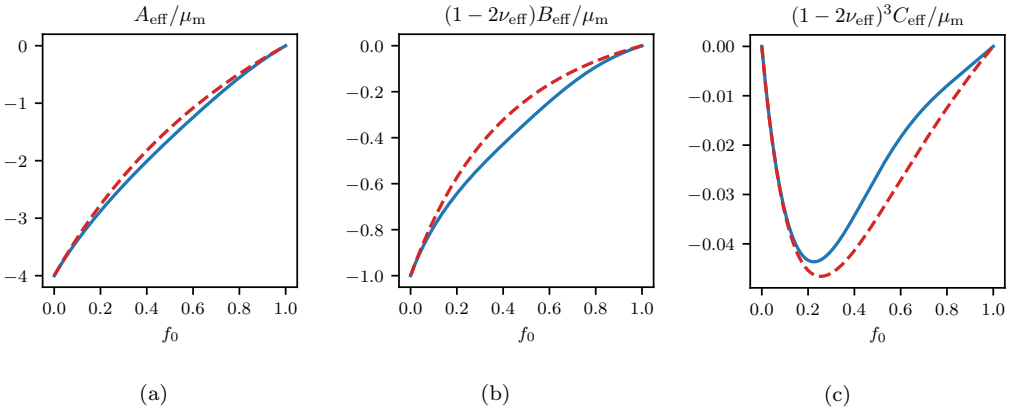

Figure 3: Effective properties of a neo-Hookean material containing voids at volume fraction f_0. The predictions based on the volume-average methodology (solid blue line) and the predictions of [19] (broken red line) are compared.

Comparison may be made with results for neo-Hookean material containing a distribution of voids presented in [23, 20]. In particular, [20] presented an analytical expression for the effective strain energy density function for spherically-symmetric deformations, i.e. in the case where the volume-averaged deformation gradient can be represented in the form $\overline{\mathbf{F}} =$

$\mathrm{diag}(\overline{J}^{1/3}, \overline{J}^{1/3}, \overline{J}^{1/3})$. To express the present results in terms of the effective strain energy density function, it is straightforward to show that if the deformation is spherically symmetric, then

$$\overline{W} = \frac{9}{8}(\overline{J}^{2/3} - 1)^2(\lambda_{\text{eff}} + \tfrac{2}{3}\mu_{\text{eff}}) + \frac{9}{8}(\overline{J}^{2/3} - 1)^3(l_{\text{eff}} + \tfrac{1}{9}n_{\text{eff}})$$

and hence, in terms of the volume fraction f_0,

$$\overline{W} = \mu\left[\frac{3(1-f_0)}{2f_0}(\overline{J}^{2/3} - 1)^2 - \frac{(1-f_0)(11+5f_0)}{8f_0^2}(\overline{J}^{2/3} - 1)^3\right] \tag{41}$$

which is identical, up to third-order in $\overline{J} - 1$, to the effective strain energy function for spherically-symmetric deformations presented in [20]. Note that the results of the method presented in [19] differ from eq. (41), as the methodology used in [19] is based on the referential volume average of the strain energy rather than the first Piola-Kirchhoff stress.

5.2. Compressible constituents

The general case of a two-phase nonlinear composite material with both phases described by the Murnaghan constitutive model (3) requires the specification of ten linear and nonlinear elastic moduli. Additionally, though there are well-known restrictions on the constants of linear isotropic elasticity (namely $K = \lambda + \frac{2}{3}\mu > 0$, $\mu > 0$) there are no accepted restrictions on the TOECs. Experimental studies on metal alloys have reported that the TOECs l, m, n are often negative, and the order of magnitude is often the same or higher than λ and μ [40], though these observations do not hold true for all materials. The above-mentioned considerations suggest that a parametric study would be prohibitively difficult and cumbersome. Instead,

Table 1: Elastic constants for a Polystyrene-particle reinforced Polycarbonate composite used by [19].

Elastic constant	Matrix	Particle
K (GPa)	3.93	4.20
μ (GPa)	0.84	1.50
l (GPa)	−50.00	−18.90
m (GPa)	−12.20	−13.30
n (GPa)	−32.00	−10.00

some numerical results for several combinations of nonlinear constituents are presented in this Section.

Examples of compressible nonlinear composites have been given in [29] and [19]; the material properties considered by these authors are listed in Tables 1 and 2. The variation in the effective TOECs with volume fraction f_0 for these composites are shown in Figs. 4 and 5. It is necessary to highlight again that the derivation of the analytical expressions neglected interactions between particles, and therefore results at non-dilute distributions must be treated with caution. Nevertheless, it can be seen from Figs. 4 and 5 that the effective nonlinear elastic moduli, unlike the linear elastic constants, may vary non-monotonically, and extrema may occur at interior points of the interval $0 < f_0 < 1$, rather than only at the endpoints. Moreover, even for a material in which the nonlinear elastic properties of the matrix are set to zero (e.g. the material given by [29]), the effective nonlinear elastic properties may vary rapidly, specifically at low particle volume fractions, see Fig. 5.

Comparisons of the theoretical predictions based on the present results,

Table 2: Elastic constants for a particulate composite proposed by [29]. The matrix phase is assumed to be linearly elastic in [29]; in the present calculations, the TOECs are taken to be zero.

Elastic constant	Matrix	Particle
K (GPa)	10.0	1.0
μ (GPa)	1.0	4.0
l (GPa)	0.0	13.0
m (GPa)	0.0	6.5
n (GPa)	0.0	-3.0

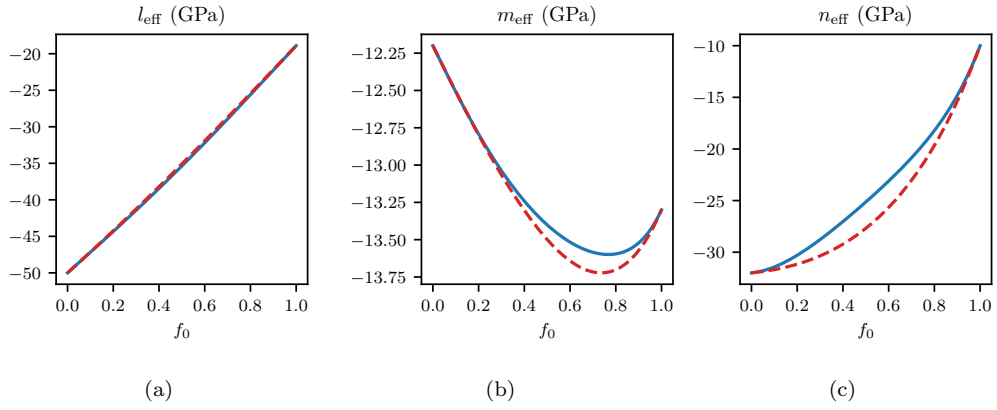

(a) (b) (c)

Figure 4: Effective properties of the Polystyrene–Polycarbonate composite considered by [19]. The predictions provided by [19] (broken red line) and the volume-average methodology (solid blue line) are compared.

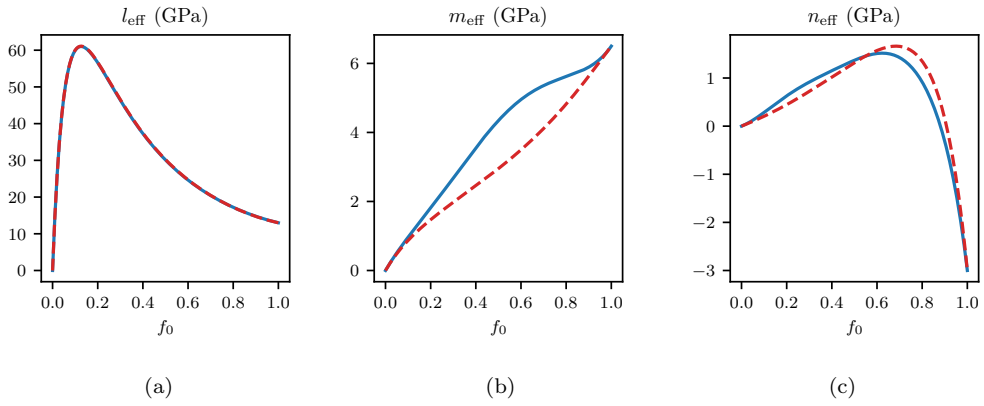

Figure 5: Effective properties of the composite medium considered by [29]. The predictions provided by [19] (broken red line) and the volume-average methodology (solid blue line) are compared.

and the strain energy perturbation method [19] are shown in Figs. 4 and 5. A simple analysis demonstrates that the Taylor expansion of both estimates with respect to the volume fraction, f_0, is identical for the linear term, and differs in higher-order terms. Thus, the estimates have the same asymptotic behaviour at $f_0 \to 0$ and this behaviour, as discussed in the Introduction, has been validated with nonlinear 3D FE simulations for $f_0 < 0.2$ [19].

It is also clearly seen from Figs. 4 and 5 that the general character of the predictions are similar: if a certain volume fraction causes an extreme value in one of the effective properties in one methodology, then the other methodology exhibits an extremum of approximately the same magnitude at approximately the same value of f_0. It is also noted that neither methodology bounds the other: depending on the elastic moduli, the functions for the effective elastic properties can intersect at certain values of f_0.

5.3. Comparison with experimental results

The literature is saturated with experimental data for TOECs of crystals, structural materials and rocks indicating a significant interest in this data from very different perspectives, e.g. design of electronic components, damage evaluation of structural materials [41], geomechanics, and oil and gas exploration methods [42]. However, there exist only limited experimental data with respect to particulate composites, specifically at various particle concentrations, which is suitable for comparison and validation purposes.

Numerical data for the linear and nonlinear elastic constants of the Al7064-SiC composite with near spherical particles (SiC) were reported by [43]. The data has been obtained using ultrasonic measurements of uniaxially stressed composite samples. It is likely that this data is affected by the fabrication process and various microstructural features differently for measurements taken at different particle concentrations. In addition, the level of micro-residual stresses for each sample would be expected to significantly affect the evaluation of the nonlinear properties, which are normally measured using the acoustoelastic effect, or wave speed changes with the applied stress.

The comparison of the current theoretical results and experimental data [43] is presented in Fig. 6 and Table 3. The linear and nonlinear properties of the composite are found using the standard least squares fitting procedure and the elastic constants of the matrix and particulate phases are compared against the linear and nonlinear properties presented in [19]. Only a slight difference between the two studies can be noted in the nonlinear elastic constants l and m.

Other possible sources of error in measurements of the effective elastic

Table 3: Numerical values for the elastic constants of the matrix and particle phases of the Al7064-SiC particulate composite reported by [43]. The presented values are obtained using a least squares fitting procedure. Note that the numerical values for all elastic constants are presented in GPa.

	Phase	λ	μ	l	m	n
Present work	Matrix	51.24	28.21	−242.13	−307.30	−381.34
	Particle	76.76	189.22	−82.16	−299.18	−682.35
Ref. [19]	Matrix	51.24	28.21	−242.13	−307.30	−381.34
	Particle	76.76	189.22	−82.28	−298.96	−682.01

properties of composites include agglomeration of inclusions, nonuniform particle dispersion within the matrix, and the interaction between the particles and the ultrasonic wave depending upon the excitation frequency. A recent experimental study which controlled and correct for these errors was performed by Belashov et al [44], investigating the effective properties of polystyrene nanocomposites reinforced by SiO_2 and Carbon Black nanofillers. The acoustoelastic technique was used to determine the higher-order elastic constants at a volume fraction of 0.2 for each reinforcement. As the results were presented for only one volume fraction, only a limited comparison is possible, but in general it appears that theoretical predictions of both the current work and [19] are broadly in agreement with the experimental results, in particular for the TOECs m and n (see Table 4).

Fig. 6 and Table 4 generally indicate that the theoretical dependencies are capable of describing experimental data, although this data is very limited as discussed above. In particular, a good correlation is obtained for some linear

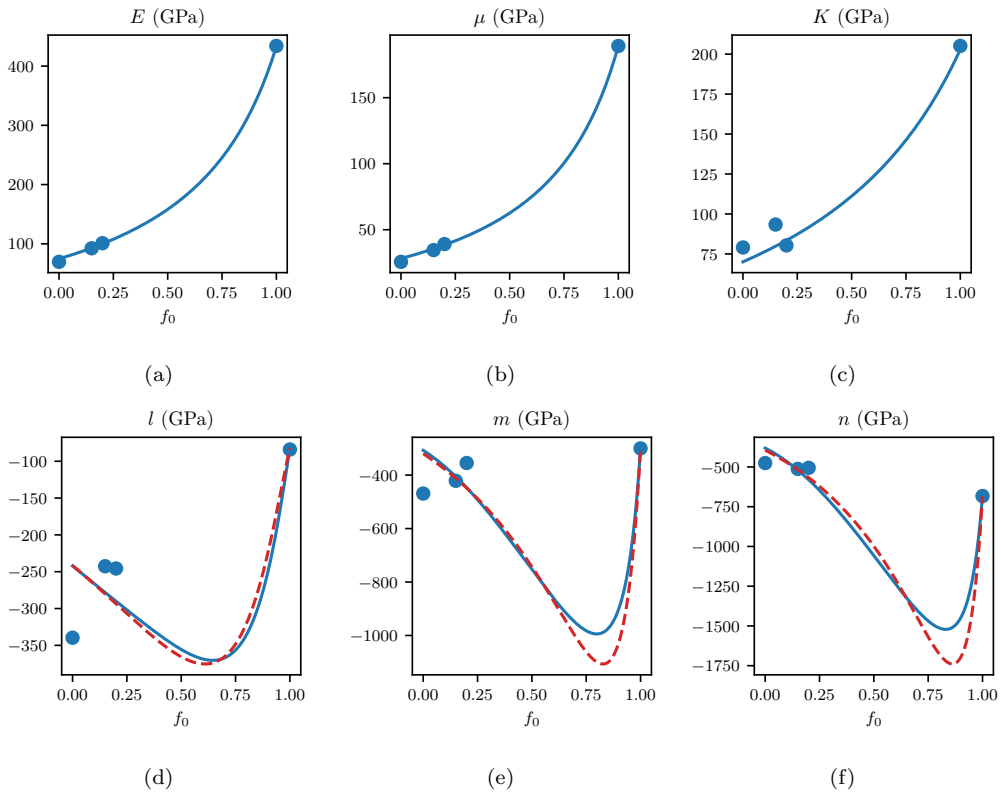

Figure 6: Least squares fit for the experimental data reported by [43] for the particulate composite with matrix Al7064 and particulate phase SiC. The predictions provided by [19] (broken red line) and the volume-average methodology (solid blue line) are compared (for the linear elastic constants, the predictions are identical).

Table 4: Experimentally-measured values for the elastic constants of the PS+20%SiO_2 and PS+20%CB nanocomposites reported by [44], as well as theoretical predictions based on the current work and [19]. Note that the numerical values for all elastic constants are presented in GPa.

Material	Method	λ	μ	l	m	n
PS+20%SiO_2	Experiment, [44]	3.28	1.55	−62.9	−15.5	−7.10
	Theory, present work	3.11	1.78	−51.5	−17.1	−9.32
	Theory, [19]	3.11	1.78	−51.8	−16.1	−8.13
PS+20%CB	Experiment, [44]	3.72	1.78	−85.3	−19.6	−5.60
	Theory, present work	3.22	1.84	−55.9	−19.3	−11.0
	Theory, [19]	3.22	1.84	−56.3	−17.6	−9.09

elastic constants (Young's moduli and shear moduli), however much worse correlation is observed for the bulk modulus. The latter can be associated with much higher bulk wave speed utilised for the experimental evaluation, which normally results in a lower resolution and larger measurement errors. The experimental data for nonlinear elastic constants is quite inconsistent, and therefore, only a general agreement between experimental and theoretical results can be stated for the conducted comparison.

6. Conclusion

In this paper, several new results have been reported which are discussed below. An axisymmetric second-order solution for a spherical particle embedded in a matrix of finite external radius has been derived for the first time in the case of weakly nonlinear material behaviour using a perturbation

expansion method. This solution obtained for finite deformations is an analogue of the linear Eshelby solution for the case of materials with spherical inclusions subjected to axisymmetric deformations [4, 5], and it converges to the classical solution for infinitesimal deformations. The finite deformation theory of elasticity is necessary as the effect of finite deformations and the contribution of the nonlinear elastic constants (TOECs) into the mechanical response is of the same order of magnitude for most structural materials and composites.

The second-order solution is then used to derive the central results of this paper, which are explicit analytical expressions for the effective nonlinear elastic moduli, based on the classical stress volume averaging methodology. These expressions have been obtained in closed form similar to linear elastic micromechanics, and have been extensively validated against previously obtained results including the strain energy perturbation method (which has been found to be in good agreement with 3D FE simulations) as well as particular cases, specifically for composites with incompressible constituents. Though both methodologies mentioned above provide quite similar results for a range of composite materials (see Section 5), one of the most notable discrepancies is that the stress-based methodology is consistent with the analytical solution for an incompressible neo-Hookean solid containing cavities reported by Hashin [23, 20]. One important restriction is that all expressions for the effective properties have been obtained for dilute distributions of the particle phase only, and using a perturbation solution, so the results for high concentration of particles, and large deformations, must be interpreted with care.

As discussed in Section 1, it is argued that current numerical procedures and methods need extensive convergence and mesh sensitivity studies when applied to the evaluation of the effective TOECs of weakly nonlinear composites, particularly in the case of the dilute distribution of the secondary phase. Moreover, the large number of independent elastic constants required to describe common structural materials make parametric computational studies unfeasible. It seems the analytical approach adopted in this work is currently the most appropriate treatment of the problem under consideration. The presented theoretical results may also stimulate the development of new numerical methods for averaging material properties by providing benchmarks for challenging cases.

The focus of future work may involve an experimental validation of the obtained theoretical expressions. Unfortunately, the authors could find only limited experimental data regarding the effective nonlinear properties of composites with different volume fractions of spherical particles, which are not sufficient for comprehensive validation of current theoretical results. The experimental evaluation of the TOECs for common metals and alloys differs from conventional testing of material properties using the stress-strain diagram. The nonlinear elastic properties are typically evaluated using the acoustoelastic effect (which describes the influence of the stress state on the speed of a propagating elastic wave) or various nonlinear effects, such as the generation of higher-order harmonics [45, 46, 47]. Both techniques are based on the generation and processing of ultrasonic wave signals. In turn, it is expected that numerous experimental techniques based on nonlinear ultrasonic bulk and guided waves are the primary research and engineering

fields which can directly benefit from the current developments. For example, the effective properties of a composite material may be tuned to produce many interesting nonlinear wave phenomena and effects. One such effect is the negation or amplification of the ultrasonic wave nonlinearities associated with finite deformations and nonlinear material properties. The appropriate constituents and volume fractions can be identified for different composite materials, and may be implemented in material design using the current theoretical framework.

Previous studies [9, 37] indicate that the third-order elastic constants are generally more sensitive to the concentration of the secondary phases in comparison to the linear elastic moduli. Therefore, the derived expressions may lay the foundation for the development of new experimental techniques e.g. to evaluate the porosity of a material or the concentration of impurities or inclusions.

Extension and generalisation of this work to distributed localised plastic deformations may provide a foundation for theoretical modelling and experimental evaluation of microscopic dislocation-driven damage, e.g. during fatigue or creep. In accordance with numerous experimental studies, the latter have a significant effect on the elastic nonlinearities [48, 49]. The use of a micromechanical model to predict damage was investigated in a recent study on syntactic foams [25]. In this study a micromechanical model combined with a phenomenological model based on experimental observations was used to predict the mechanical response of syntactic foams due to fracture of buckling of the constituents. Such methods may prove to be useful in extending the current model to describe the effect of microscopic damage accumulation

on the overall behaviour, though it remains a formidable task to identify the link between material nonlinearities on the structural scale and microscopic changes due to mechanical damage.

Another promising direction is the evaluation of effective properties of porous materials saturated or partially saturated with a fluid instead of solid particles. This problem has numerous applications in civil engineering, geomechanics as well as in oil and gas exploration methods. However, the derivation of the effective properties in this case is more complex as it has to be based on the nonlinear theory for porous elastic solids, which require more material constants to describe the interaction between the solid and liquid constituencies. Therefore, the current work can be considered as a starting point for the derivation of effective properties for saturated porous media.

Acknowledgements

The authors would like to thank Dr. L. R. Francis Rose for many helpful discussions and comments during the preparation of this article.

Funding

This research was partially supported by the Australian Government through the Australian Research Council's Discovery Projects funding scheme (project DP200102300); and the Australian Government Research Training Program (RTP) Scholarship.

Appendix A. Material and spatial basis

The material configuration may be described by the spherical coordinates (R, Θ, Φ), where Φ is the azimuthal angle, and Θ is the polar angle. Similarly, the spatial configuration may be described by the spherical coordinates (r, θ, ϕ). The physical basis vectors for the spherical coordinates of the material coordinate system are

$$\mathbf{d}_R = \sin\Theta\cos\Phi\mathbf{d}_X + \sin\Theta\sin\Phi\mathbf{d}_Y + \cos\Theta\mathbf{d}_Z \tag{A.1a}$$

$$\mathbf{d}_\Theta = \cos\Theta\cos\Phi\mathbf{d}_X + \cos\Theta\sin\Phi\mathbf{d}_Y - \sin\Theta\mathbf{d}_Z \tag{A.1b}$$

$$\mathbf{d}_\Phi = -\sin\Theta\sin\Phi\mathbf{d}_X + \sin\Theta\cos\Phi\mathbf{d}_Y \tag{A.1c}$$

where the basis vectors $(\mathbf{d}_X, \mathbf{d}_Y, \mathbf{d}_Z)$ form a Cartesian basis for the material body.

Appendix B. Second-order stress and displacement solutions

The second-order term $\mathbf{T}'(\mathbf{u}_1)$ in eq. (12) has the form

$$\begin{aligned}\mathbf{T}'(\mathbf{u}_1) = \boldsymbol{\sigma}(\mathbf{u}_1)\nabla\mathbf{u}_1 + \left[\lambda\boldsymbol{\omega}\cdot\boldsymbol{\omega} + \left(l - m + \tfrac{1}{2}n\right)\vartheta^2 + \tfrac{1}{2}\left(\lambda + 2m - n\right)\right]\mathbf{G} \\ + (2m - n)\vartheta\boldsymbol{\varepsilon}(\mathbf{u}_1) + n\boldsymbol{\varepsilon}(\mathbf{u}_1)^2 + \mu\nabla\mathbf{u}_1(\nabla\mathbf{u}_1)^T\end{aligned}$$

where

$$\begin{aligned}\boldsymbol{\varepsilon}(\mathbf{u}) &= \tfrac{1}{2}\nabla\mathbf{u} + \tfrac{1}{2}(\nabla\mathbf{u})^T \\ \vartheta &= \mathrm{Div}\,\mathbf{u}_1 \\ \boldsymbol{\omega} &= \tfrac{1}{2}\mathrm{Curl}\,\mathbf{u}_1.\end{aligned}$$

Appendix C. Linear elastic solution

The linear elasticity problem presented in Section 3.2 leads to the following system of linear equations, where $f_0 = R_i^3/R_e^3$,

$$\frac{3(\lambda_m + 2\mu_m)}{\lambda_m + \mu_m} B_1^{(m)} - \frac{3K_p + 4\mu_m}{\lambda_p + \mu_p} B_1^{(p)} = 0$$

$$\left(\frac{1}{\nu_m} - 1\right) A_4^{(m)} - \frac{4\mu_m(7 - 10\nu_p) + \mu_p(7 + 5\nu_p)}{35\nu_p\mu_p} A_4^{(p)} = 0$$

$$B_3^{(m)} + \frac{7}{4\nu_m} A_4^{(m)} = 0$$

$$B_3^{(p)} + \frac{7}{4\nu_p} A_4^{(p)} = 0$$

$$\frac{5}{3}\mu_m \left(\frac{A_2^{(m)}}{\mu_m} - \frac{A_2^{(p)}}{\mu_p}\right) + \mu_m \left(\frac{B_3^{(m)}}{\mu_m} - \frac{B_3^{(p)}}{\mu_p}\right) + \frac{5}{3} F_0^{(m)} + G_1^{(m)} = 0$$

$$A_2^{(m)} - A_2^{(p)} - 2(B_1^{(m)} - B_1^{(p)}) + \frac{3}{4}(A_4^{(m)} - A_4^{(p)}) + 4F_0^{(m)} + 6F_2^{(m)} + 2(5 - 3\nu_m) G_1^{(m)} = 0$$

$$\frac{7 + 5\nu_m}{16\nu_m} A_4^{(m)} - \frac{7 + 5\nu_p}{16\nu_p} A_4^{(p)} + \frac{5}{2} F_2^{(m)} + G_1^{(m)} = 0$$

$$A_2^{(m)} - (1 - 2\nu_m) B_1^{(m)} - \frac{3}{2} f_0^{-2/3} A_4^{(m)} - \frac{1}{2} f_0 F_0^{(m)} - \frac{3}{2} f_0^{5/3} F_2^{(m)} - \frac{1}{2}(5 - 4\nu_m) f_0 G_1^{(m)} = \mu_m$$

$$-\frac{1}{2} A_2^{(m)} + \frac{3}{4} f_0^{-2/3} A_4^{(m)} - \frac{1}{2} f_0 F_0^{(m)} + \frac{3}{4} f_0^{5/3} F_2^{(m)} = \alpha\mu_m$$

$$\frac{3(2\lambda_m + 7\mu_m)}{4\lambda_m} f_0^{-2/3} A_4^{(m)} - \frac{15}{4} f_0^{5/3} F_2^{(m)} - \frac{3}{2} f_0 G_1^{(m)} = 0$$

$$B_1^{(m)} - \frac{(1 + 2\alpha)(\lambda_m + \mu_m)(3K_p + 4\mu_m)}{3f_0(K_p - K_m) - (3K_p + 4\mu_m)} = 0$$

which may be solved using standard techniques to identify each of the coefficients in the linear elastic solution.

Appendix D. Second-order inhomogeneous solution

The second-order elastic problem specified by eqs. (16b), (17b) and (18b) features inhomogeneous terms, which requires the development of a partic-

ular solution to the elasticity problem. As this procedure is not a routine calculation in linear elasticity, complete expressions for the potential function ζ and vector function $\mathbf{w}$ in each phase of the composite are provided below.

Appendix D.1. Matrix

In the matrix phase, the particular solution, eq. (25), is formed from the following expressions:

$$\zeta^{(m)} = \frac{3\lambda_m + 9\mu_m + 6m_m}{\lambda_m + 2\mu_m}\zeta_1 + \frac{1}{\mu_m(1-\nu_m)}\zeta_2 \tag{D.1a}$$

$$\begin{aligned}\zeta_1 = {} & \alpha_1[F_0^{(m)}]^2 R^{-4} + \alpha_2[3A_2^{(m)} - 2(1-2\nu_m)B_1^{(m)}]A_4^{(m)} R^4 + \alpha_3 A_4^{(m)} F_0^{(m)} R\cos^2\Theta \\ & + 4\alpha_4 F_0^{(m)} F_2^{(m)} R^{-6} P_2(\cos\Theta) + (\alpha_{5,1} + \alpha_{5,2}\cos 2\Theta) F_0^{(m)} G_1^{(m)} R^{-4} \\ & + (\alpha_6[3A_2^{(m)} - 2(1-2\nu_m)B_1^{(m)}]G_1^{(m)} + \alpha_7 A_4^{(m)} F_2^{(m)}) R^{-1} P_4(\cos\Theta) \\ & + (\alpha_{8,1} + \alpha_{8,2}\cos 2\Theta + \alpha_{8,3}\cos 4\Theta) F_2^{(m)} G_1^{(m)} R^{-6} \\ & + \alpha_9[F_2^{(m)}]^2 R^{-8}(1 + \tfrac{12}{15}\cos 2\Theta + \tfrac{1}{3}\cos 4\Theta)\end{aligned} \tag{D.1b}$$

$$\begin{aligned}\zeta_2 = {} & (\beta_{1,1} + \beta_{1,2}\cos 2\Theta + \beta_{1,3}\cos 4\Theta) A_4^{(m)} G_1^{(m)} R + (\beta_{2,1} + \beta_{2,2}\cos 2\Theta)[A_4^{(m)}]^2 R^6 \\ & + (\beta_{3,1} + \beta_{3,2}\cos 2\Theta + \beta_{3,3}\cos 4\Theta)[G_1^{(m)}]^2 R^{-4}\end{aligned} \tag{D.1c}$$

$$\begin{aligned}w_R^{(m)} = {} & \left(a_1^{(m)} R^7 [A_4^{(m)}]^2 + a_2^{(m)} R^{-3} F_0^{(m)} G_1^{(m)}\right) P_2(\cos\Theta) \\ & + \left(a_3^{(m)} A_4^{(m)} F_2^{(m)} + a_4^{(m)} A_2^{(m)} G_1^{(m)} + a_5^{(m)} B_1^{(m)} G_1^{(m)} + a_6^{(m)} G_1^{(m)}\right) P_4(\cos\Theta) \\ & + a_7^{(m)} R^{-5} F_2^{(m)} G_1^{(m)}[P_2(\cos\Theta) - \tfrac{9}{2}P_4(\cos\Theta)] + R^{-3}[G_1^{(m)}]^2[a_8^{(m)} P_2(\cos\Theta) + a_9^{(m)} P_4(\cos\Theta)] \\ & + R^2 A_4^{(m)} F_0^{(m)}[a_{10}^{(m)} + a_{11}^{(m)} P_2(\cos\Theta)] + R^2 A_4^{(m)} G_1^{(m)}[a_{12}^{(m)} + a_{13}^{(m)} P_2(\cos\Theta) + a_{14}^{(m)} P_4(\cos\Theta)]\end{aligned} \tag{D.1d}$$

$$w_{\Theta}^{(m)} = \Big(b_1^{(m)} F_0^{(m)} - \tfrac{1}{6} R^{-3} a_2^{(m)} F_0^{(m)} G_1^{(m)} + R^5 b_3^{(m)} A_4^{(m)} A_2^{(m)} + R^5 b_4^{(m)} A_4^{(m)} B_1^{(m)} + \tfrac{2}{3} R^2 a_{11}^{(m)} A_4^{(m)} F_0^{(m)} \Big)$$
$$+ R^2 [\tfrac{2}{3} a_{13}^{(m)} P_2'(\cos\Theta) + \tfrac{1}{5} a_{14}^{(m)} P_4'(\cos\Theta)] A_4^{(m)} G_1^{(m)} + R^7 [\tfrac{3}{2} a_1^{(m)} P_2'(\cos\Theta) + b_9^{(m)} P_4'(\cos\Theta)] [A_4^{(m)}$$
$$+ [b_{10}^{(m)} P_2'(\cos\Theta) - \tfrac{1}{35} R_i^2 a_{11}^{(m)} P_4'(\cos\Theta)] A_4^{(m)} F_2^{(m)} + [b_{12}^{(m)} P_2'(\cos\Theta) + \tfrac{1}{10} a_5^{(m)} P_4'(\cos\Theta)] B_1^{(m)} G_1^{(r}$$
$$+ \tfrac{9}{7} R_i^2 R^{-2} b_1^{(m)} F_2^{(m)} P_4'(\cos\Theta) + \tfrac{1}{10} a_4^{(m)} A_2^{(m)} G_1^{(m)} P_4'(\cos\Theta)$$
$$- R^{-3} [\tfrac{1}{6} a_8^{(m)} P_2'(\cos\Theta) + \tfrac{1}{20} a_9^{(m)} P_4'(\cos\Theta)] [G_1^{(m)}]^2 + \tfrac{21}{64} R^{-5} a_7^{(m)} \sin 2\Theta (1 - 9\cos 2\Theta) F_2^{(m)} G_1^{(m)}$$
$$+ [b_{19}^{(m)} P_2'(\cos\Theta) + b_{20}^{(m)} P_4'(\cos\Theta)] A_2^{(m)} G_1^{(m)} + [b_{21}^{(m)} P_2'(\cos\Theta) + b_{22}^{(m)} P_4'(\cos\Theta)] B_1^{(m)} G_1^{(m)} \tag{D.1e}$$

where $P_n'(\cos\Theta) = \frac{d}{d\Theta}[P_n(\cos\Theta)]$, and the coefficients in eqs. (D.1) may be calculated using eq. 14.

Appendix D.2. Particle

In the particle phase, the particular solution, eq. (28), is formed from the following expressions:

$$\zeta^{(p)} = R^4 \alpha_1^{(p)} A_2^{(p)} A_4^{(p)} - \tfrac{2}{3}(1 - 2\nu_p) R^4 \alpha_1^{(p)} A_4^{(p)} B_1^{(p)} + R^6 [\alpha_{2,1}^{(p)} + \alpha_{2,2}^{(p)} P_2(\cos\Theta)] [A_4^{(p)}]^2 \tag{D.2a}$$

$$w_R^{(p)} = R^7 a_1^{(p)} [A_4^{(p)}]^2 P_2(\cos\Theta) \tag{D.2b}$$

$$w_{\Theta}^{(p)} = R^5 b_1^{(p)} B_1^{(p)} A_4^{(p)} P_2'(\cos\Theta) + R^5 b_2^{(p)} A_2^{(p)} A_4^{(p)} P_2'(\cos\Theta) + R^7 [b_{3,1}^{(p)} P_2'(\cos\Theta) + b_{3,2}^{(p)} P_4'(\cos\Theta)] [A_4^{(p)}]^2 \tag{D.2c}$$

where the coefficients in eqs. (D.2) may be calculated using eq. 14.

Appendix E. Example values of the displacement coefficients

The following tables provide the values of the displacement solution coefficients in eqs. (20), (22), (24) and (27) for a composite medium with elastic

properties given in Table 1, and with $\alpha = 0$ and $f_0 = 0.008$. The coefficients in the linear potentials are shown in Table E.5, and Table E.6 shows the coefficients in the second-order potentials. For different material properties or volume fractions, the displacement potential coefficients may be calculated using the Python code provided as supplementary data.

Table E.5: Numerical values for the linear displacement potential coefficients, eqs. (20) and (22), for $\alpha = 0$, $f_0 = 0.008$, and using the material properties presented in Table 1.

Coefficient	Value
$A_4^{(m)}/\mu_m$	5.3483×10^{-5}
$A_2^{(m)}/\mu_m$	4.6270×10^{-3}
$A_4^{(p)}/\mu_m$	5.6988×10^{-5}
$A_2^{(p)}/\mu_m$	-2.4165×10^{-1}
$B_3^{(m)}/\mu_m$	-2.3385×10^{-4}
$B_1^{(m)}/\mu_m$	-5.0139
$B_3^{(p)}/\mu_m$	-2.9295×10^{-4}
$B_1^{(p)}/\mu_m$	-5.3134
$F_0^{(m)}/\mu_m$	-3.3550×10^{-1}
$F_2^{(m)}/\mu_m$	-1.3039×10^{-1}
$G_1^{(m)}/\mu_m$	3.2598×10^{-1}

Appendix F. Coefficients in the effective TOECs

The expressions for the effective TOECs derived using the volume averaging methodology involve the following coefficients:

$$h_0 = 3K_p + 4\mu_m \tag{F.1a}$$

Table E.6: Numerical values for the normalised second-order displacement potential coefficients, eqs. (24) and (27), for $\alpha = 0$, $f_0 = 0.008$, and using the material properties presented in Table 1.

Coefficient	Value
$A_7^{(m)}/\mu_m$	-7.4067×10^{-6}
$A_7^{(p)}/\mu_m$	8.5532×10^{-3}
$A_5^{(m)}/\mu_m$	6.2224×10^{-4}
$A_5^{(p)}/\mu_m$	-1.8191×10^{-2}
$B_6^{(m)}/\mu_m$	2.2626×10^{-5}
$B_6^{(p)}/\mu_m$	-2.7987×10^{-2}
$F_5^{(m)}/\mu_m$	-1.3655
$G_4^{(m)}/\mu_m$	9.7105×10^{-1}
$A_3^{(p)}/\mu_m$	6.0950
$B_2^{(m)}/\mu_m$	-3.3297×10^{-1}
$B_4^{(m)}/\mu_m$	-4.2096×10^{-3}
$B_4^{(p)}/\mu_m$	1.3703×10^{-1}
$F_3^{(m)}/\mu_m$	-6.5165×10^{-1}
$G_2^{(m)}/\mu_m$	3.0760
$A_3^{(m)}/\mu_m$	-4.8620×10^{-2}
$B_2^{(p)}/\mu_m$	3.9207×10^{1}
$F_1^{(m)}/\mu_m$	1.1985

$$k_0 = 5\mu_m(3K_m + 4\mu_m) + 6(K_m + 2\mu_m)(\mu_p - \mu_m) \tag{F.1b}$$

$$\begin{aligned} p_{1,0} = {} & 20\mu_m(3K_m + 4\mu_m)(3K_m + 8\mu_m) \\ & + (81K_m^2 + 324K_m\mu_m + 364\mu_m^2)(\mu_p - \mu_m) \end{aligned} \tag{F.1c}$$

$$p_{2,0} = [5(3K_m + 4\mu_m)^3 - 7\mu_m(3K_m + 4\mu_m)^2 + 9\mu_m^2(24K_m + 25\mu_m)](K_p - K_m)(\mu_p - \mu_m) + 5K_m(3K_m + 4\mu_m)[(3K_m + 4\mu_m)^2 + 6\mu_m^2](\mu_p - \mu_m) + 60\mu_m^3(3K_m + 4\mu_m)(K_p - K_m) \tag{F.1d}$$

$$p_{3,0} = 25\mu_m^2(3K_m + 4\mu_m)^3 + 36(K_m + 2\mu_m)^2(\mu_p - \mu_m)^2[3K_m + 4\mu_m + 3(K_p - K_m)] + 180\mu_m(K_p - K_m)(K_m + 2\mu_m)(3K_m + 4\mu_m)(\mu_p - \mu_m) + 15\mu_m(3K_m + 4\mu_m)^2[4(K_m + 2\mu_m)(\mu_p - \mu_m) + 5\mu_m(K_p - K_m)] \tag{F.1e}$$

$$p_{3,1} = 120\mu_m^2(3K_m + 4\mu_m)(K_p - K_m)(\mu_p - \mu_m) + 6(3K_m + 4\mu_m)[(3K_m + 4\mu_m)^2 - 8K_m\mu_m](\mu_p - \mu_m)^2 + 6[3(3K_m + 4\mu_m)^2 + 2\mu_m(3K_m + 35\mu_m)](K_p - K_m)(\mu_p - \mu_m)^2 \tag{F.1f}$$

$$p_{4,0} = -10\mu_m(3K_m + 4\mu_m)[9K_m^2 + 24K_m\mu_m + 28\mu_m^2] - [10(3K_m + 4\mu_m)^3 + \mu_m(3K_m + 4\mu_m)^2 + 6\mu_m^2(42K_m + 55\mu_m)](\mu_p - \mu_m) \tag{F.1g}$$

$$p_{5,0} = 7[\mu_m(9K_m + 8\mu_m) + 6\mu_p(K_m + 2\mu_m)]^3 \tag{F.1h}$$

$$p_{5,1} = 15\mu_m(\mu_p - \mu_m)^2(3K_m + 4\mu_m)\left(63K_m^2 - 48K_m\mu_m - 128\mu_m^2\right) + (\mu_p - \mu_m)^3(1026K_m^3 + 1161K_m^2\mu_m - 3168K_m\mu_m^2 - 3272\mu_m^3). \tag{F.1i}$$

References

[1] W. Voigt, Ueber die Beziehung zwischen den beiden Elasticitätsconstanten isotroper Körper, Annalen der Physik 274 (12) (1889)

573–587. doi:10.1002/andp.18892741206.

[2] A. Reuss, Berechnung der Fließgrenze von Mischkristallen auf Grund der Plastizitätsbedingung für Einkristalle, ZAMM - Zeitschrift für Angewandte Mathematik und Mechanik 9 (1) (1929) 49–58. doi:10.1002/zamm.19290090104.

[3] Z. Hashin, S. Shtrikman, Note on a variational approach to the theory of composite elastic materials, Journal of the Franklin Institute 271 (4) (1961) 336–341. doi:10.1016/0016-0032(61)90032-1.

[4] J. D. Eshelby, The elastic field outside an ellipsoidal inclusion, Proceedings of the Royal Society of London. Series A. Mathematical and Physical Sciences 252 (1271) (1959) 561–569. doi:10.1098/rspa.1959.0173.

[5] J. D. Eshelby, Elastic inclusions and inhomogeneities, Vol. 2 of Progress in Solid Mechanics, 1961, pp. 89–140.

[6] T. Mori, K. Tanaka, Average stress in matrix and average elastic energy of materials with misfitting inclusions, Acta Metallurgica 21 (5) (1973) 571–574. doi:10.1016/0001-6160(73)90064-3.

[7] R. Hill, A self-consistent mechanics of composite materials, Journal of the Mechanics and Physics of Solids 13 (4) (1965) 213–222. doi:10.1016/0022-5096(65)90010-4.

[8] R. Christensen, K. Lo, Solutions for effective shear properties in three phase sphere and cylinder models, Journal of the Mechanics and Physics of Solids 27 (4) (1979) 315–330. doi:10.1016/0022-5096(79)90032-2.

[9] R. W. Ogden, On the overall moduli of non-linear elastic composite materials, Journal of the Mechanics and Physics of Solids 22 (6) (1974) 541–553. doi:10.1016/0022-5096(74)90033-7.

[10] R. W. Ogden, Extremum principles in non-linear elasticity and their application to composites—I, International Journal of Solids and Structures 14 (4) (1978) 265–282. doi:10.1016/0020-7683(78)90037-9.

[11] P. Ponte Castañeda, The overall constitutive behaviour of nonlinearly elastic composites, Proceedings of the Royal Society of London. A. Mathematical and Physical Sciences 422 (1862) (1989) 147–171. doi:10.1098/rspa.1989.0023.

[12] R. Hill, On constitutive macro-variables for heterogeneous solids at finite strain, Proceedings of the Royal Society of London. A. Mathematical and Physical Sciences 326 (1565) (1972) 131–147. doi:10.1098/rspa.1972.0001.

[13] S. Nemat-Nasser, Averaging theorems in finite deformation plasticity, Mechanics of Materials 31 (8) (1999) 493–523. doi:10.1016/S0167-6636(98)00073-8.

[14] S. Saeb, P. Steinmann, A. Javili, Aspects of Computational Homogenization at Finite Deformations: A Unifying Review From Reuss' to Voigt's Bound, Applied Mechanics Reviews 68 (5) (sep 2016). doi:10.1115/1.4034024.

[15] T. Nakamura, O. Lopez-Pamies, A finite element approach to study cavitation instabilities in non-linear elastic solids under general loading

conditions, International Journal of Non-Linear Mechanics 47 (2) (2012) 331–340. doi:10.1016/j.ijnonlinmec.2011.07.007.

[16] S. Ghosh, K. Lee, P. Raghavan, A multi-level computational model for multi-scale damage analysis in composite and porous materials, International Journal of Solids and Structures 38 (14) (2001) 2335–2385. doi:10.1016/S0020-7683(00)00167-0.

[17] Y. Cai, L. Xu, G. Cheng, Novel numerical implementation of asymptotic homogenization method for periodic plate structures, International Journal of Solids and Structures 51 (1) (2014) 284–292. doi:https://doi.org/10.1016/j.ijsolstr.2013.10.003.

[18] V. Lefèvre, A. Garnica, O. Lopez-Pamies, A WENO finite-difference scheme for a new class of Hamilton-Jacobi equations in nonlinear solid mechanics, Computer Methods in Applied Mechanics and Engineering 349 (2019) 17–44. doi:10.1016/j.cma.2019.02.008.

[19] A. A. Semenov, Y. M. Beltukov, Nonlinear elastic moduli of composite materials with nonlinear spherical inclusions dispersed in a nonlinear matrix, International Journal of Solids and Structures 191-192 (2020) 333–340. doi:10.1016/j.ijsolstr.2020.01.016.

[20] B. Shrimali, V. Lefèvre, O. Lopez-Pamies, A simple explicit homogenization solution for the macroscopic elastic response of isotropic porous elastomers, Journal of the Mechanics and Physics of Solids 122 (2019) 364–380. doi:10.1016/j.jmps.2018.09.026.

[21] H. Chen, X. Zhao, X. Lu, G. Kassab, Non-linear micromechanics of soft tissues, International Journal of Non-Linear Mechanics 56 (2013) 79–85. doi:10.1016/j.ijnonlinmec.2013.03.002.

[22] J. E. Marsden, T. J. R. Hughes, Mathematical Foundations of Elasticity, New York, 1994.

[23] Z. Hashin, Large isotropic elastic deformation of composites and porous media, International Journal of Solids and Structures 21 (7) (1985) 711–720. doi:10.1016/0020-7683(85)90074-5.

[24] O. Lopez-Pamies, M. I. Idiart, An Exact Result for the Macroscopic Response of Porous Neo-Hookean Solids, Journal of Elasticity 95 (1-2) (2009) 99–105. doi:10.1007/s10659-009-9193-5.

[25] B. Shrimali, W. J. Parnell, O. Lopez-Pamies, A simple explicit model constructed from a homogenization solution for the large-strain mechanical response of elastomeric syntactic foams, International Journal of Non-Linear Mechanics 126 (July) (2020) 103548. doi:10.1016/j.ijnonlinmec.2020.103548.

[26] B. Shrimali, K. Ghosh, O. Lopez-Pamies, The Nonlinear Viscoelastic Response of Suspensions of Vacuous Bubbles in Rubber: I — Gaussian Rubber with Constant Viscosity, Journal of Elasticity (nov 2021). doi:10.1007/s10659-021-09868-y.

[27] K. Ghosh, B. Shrimali, A. Kumar, O. Lopez-Pamies, The nonlinear viscoelastic response of suspensions of rigid inclusions in rubber: I—Gaussian rubber with constant viscosity, Journal of the Mechanics

and Physics of Solids 154 (May) (2021) 104544. doi:10.1016/j.jmps.2021.104544.

[28] B. Shrimali, M. Pezzulla, S. Poincloux, P. M. Reis, O. Lopez-Pamies, The remarkable bending properties of perforated plates, Journal of the Mechanics and Physics of Solids 154 (May) (2021) 104514. doi:10.1016/j.jmps.2021.104514.

[29] S. Giordano, P. L. Palla, L. Colombo, Nonlinear elastic Landau coefficients in heterogeneous materials, EPL (Europhysics Letters) 83 (6) (2008) 66003. doi:10.1209/0295-5075/83/66003.

[30] C. Truesdell, W. Noll, The Non-Linear Field Theories of Mechanics, Springer Berlin Heidelberg, Berlin, Heidelberg, 2004, pp. 1–579. doi:10.1007/978-3-662-10388-3_1.

[31] F. D. Murnaghan, Finite Deformations of an Elastic Solid, American Journal of Mathematics 59 (2) (1937) 235. doi:10.2307/2371405.

[32] C. Reina, B. Li, K. Weinberg, M. Ortiz, A micromechanical model of distributed damage due to void growth in general materials and under general deformation histories, International Journal for Numerical Methods in Engineering 93 (6) (2013) 575–611. doi:10.1002/nme.4397.

[33] F. D. Murnaghan, Finite deformation of an elastic solid, Applied mathematics series, John Wiley & Sons, Inc., New York, 1951.

[34] A. I. Lurie, A. Belyaev, Theory of Elasticity, Foundations of Engineering Mechanics, Springer Berlin Heidelberg, Berlin, Heidelberg, 2005. doi:10.1007/978-3-540-26455-2.

[35] A. E. H. Love, A Treatise on the Mathematical Theory of Elasticity, 4th Edition, Dover Publications, New York, 1927.

[36] J. R. Barber, Displacement Function Solutions, in: J. R. Barber (Ed.), Elasticity, Springer Netherlands, Dordrecht, 2010, pp. 321–332. doi:10.1007/978-90-481-3809-8_20.

[37] J. Vidler, A. Kotousov, C.-T. Ng, Effect of randomly distributed voids on effective linear and nonlinear elastic properties of isotropic materials, International Journal of Solids and Structures 216 (2021) 83–93. doi:10.1016/j.ijsolstr.2021.01.009.

[38] D. Gross, T. Seelig, Micromechanics and homogenization, Springer Berlin Heidelberg, Berlin, Heidelberg, 2011, pp. 229–299. doi:10.1007/978-3-642-19240-1_8.

[39] M. Destrade, R. W. Ogden, On the third- and fourth-order constants of incompressible isotropic elasticity, The Journal of the Acoustical Society of America 128 (6) (2010) 3334–3343. arXiv:1301.7448, doi:10.1121/1.3505102.

[40] R. T. Smith, R. Stern, R. W. B. Stephens, Third-Order Elastic Moduli of Polycrystalline Metals from Ultrasonic Velocity Measurements, The Journal of the Acoustical Society of America 40 (5) (1966) 1002–1008. doi:10.1121/1.1910179.

[41] A. Tabiei, W. Yi, R. Goldberg, Non-linear strain rate dependent micro-mechanical composite material model for finite element impact and

crashworthiness simulation, International Journal of Non-Linear Mechanics 40 (7) (2005) 957–970. doi:10.1016/j.ijnonlinmec.2004.10.004.

[42] A. P. Suvorov, Role of fluid phase in compression of nonlinear elastic fluid-saturated porous medium, International Journal of Non-Linear Mechanics 131 (February) (2021) 103697. doi:10.1016/j.ijnonlinmec.2021.103697.

[43] P. A. Foltyn, K. Ravi-Chandar, K. Salama, Effects of Second-Phase on the Nonlinear Behavior of Metal Matrix Composites, in: Nondestructive Characterization of Materials VI, Springer US, Boston, MA, 1994, pp. 733–739. doi:10.1007/978-1-4615-2574-5_93.

[44] A. Belashov, Y. Beltukov, O. Moskalyuk, I. Semenova, Relative variations of nonlinear elastic moduli in polystyrene-based nanocomposites, Polymer Testing 95 (2021) 107132. arXiv:2005.01061, doi:10.1016/j.polymertesting.2021.107132.

[45] J. M. Hughes, J. Vidler, C. T. Ng, A. Khanna, M. Mohabuth, L. F. Rose, A. Kotousov, Comparative evaluation of in situ stress monitoring with Rayleigh waves, Structural Health Monitoring 18 (1) (2019) 205–215. doi:10.1177/1475921718798146.

[46] M. Mohabuth, A. Khanna, J. Hughes, J. Vidler, A. Kotousov, C. T. Ng, On the determination of the third-order elastic constants of homogeneous isotropic materials utilising Rayleigh waves, Ultrasonics 96 (2019) 96–103. doi:10.1016/j.ultras.2019.02.006.

[47] J. M. Hughes, A. Kotousov, C.-T. Ng, Generation of higher harmonics with the fundamental edge wave mode, Applied Physics Letters 116 (10) (2020) 101904. doi:10.1063/1.5142416.

[48] K. H. Matlack, J. Y. Kim, L. J. Jacobs, J. Qu, Review of Second Harmonic Generation Measurement Techniques for Material State Determination in Metals, Journal of Nondestructive Evaluation 34 (1) (2015) 273. doi:10.1007/s10921-014-0273-5.

[49] C. J. Lissenden, Nonlinear ultrasonic guided waves—Principles for nondestructive evaluation, Journal of Applied Physics 129 (2) (2021) 021101. doi:10.1063/5.0038340.